between cells [1,2], and E-cadherin is the form most strongly expressed in epithelial cells. Cadherins form a complex with cytoplasmic proteins, known collectively as catenins. This molecular complex, together with other cytoskeletal components such as actin, constitutes the intercellular adherence junction [2–4]. The catenins are classified into two groups, α-catenins and β-catenins, and the latter group includes plakoglobin and *Drosophila* Armadillo protein as well as β-catenin itself [5,6]. Plakoglobin is isolated from the desmosomal fraction [7] and is present in both desmosomes and adherence junctions [8], and may therefore be a common regulatory molecule in cell junctions.

Cadherin-mediated cell adhesion acts as a suppressor of the invasion of cancer cells in vitro [9–11], and dysfunction of the E-cadherin system correlates with cancer cell invasion in human cancers [12,13]. The role of α-catenin in the cadherin adhesion system has been revealed by studies with cancer cells. The human lung cancer cell line PC9 expresses an aberrant α-catenin mRNA and shows very loose cell–cell association [14,15]. PC9 cells become much more closely associated and acquire an epithelioid arrangement after transfection with cDNA for a subtype of α-catenin and αN-catenin [16]. These results suggest that α-catenin is indispensable for cadherin-mediated cell–cell adhesion.

Previous immunohistochemical studies have revealed many examples of reduced and/or heterogeneous expression of E-cadherin [17–19] and α-catenin [20] in undifferentiated invasive cancers, and impaired expression of E-cadherin or α-catenin has been reported to be associated with high incidences of lymph node metastasis of human breast [21], esophageal [22], and head and neck [23] cancers. However, there have been few studies on the relationship between reduced E-cadherin expression and the prognosis of cancer patients [24–28].

The role of β-catenin and plakoglobin in determining the fate of cells has been suggested by work on a *Drosophila* homologue of this protein, Armadillo [29,30]. Moreover, it has been revealed that the association between E-cadherin and α-catenin is mediated by β-catenin [31], and that β-catenin in turn mediates the interactions of the cadherin–catenin complex with the c-erbB-2 gene product and epidermal growth factor receptor (EGF-R) [32–34]. A tumor suppressor gene product, APC protein, has been shown to interact with β-catenin and plakoglobin and to play important roles in the E-cadherin-mediated cell adhesion system and to participate in tumor invasion and metastasis.

In a previous study, we divided primary lung cancers into two groups on the basis of their expression of E-cadherin and catenins, as detected by immunohistochemistry [35]. In addition, we demonstrated a close relationship between E-cadherin-associated cell–cell adhesion, catenins, and cytologic features, in particular the formation of cellular clusters and the frequency of solitary cells. Preoperative evaluation of both cytologic features and E-cadherin-associated cell–cell adhesion may be useful for predicting the malignant characteristics of lung cancer [36].

E-cadherin and α-catenin, and also β-catenin and plakoglobin, play important roles in the cadherin-mediated cell adhesion system in various cancers. However, in the context of carcinogenesis of the bronchial epithelium, expression of E-cadherin, α-catenin, β-catenin, and plakoglobin in intrabronchial precancerous lesions has not yet been reported. In order to investigate a possible dysfunction of the E-cadherin-mediated cell adhesion system in intrabronchial lesions, we used immunohistochemistry to examine the expression of E-cadherin, α-catenin, β-catenin, and plakoglobin in biopsy specimens.

2. Materials and methods

2.1. Biopsy specimens

The biopsy samples were obtained from 109 patients with intrabronchial lesions resected between 1991 and 2000 at the Department of Surgery of Tokyo Medical University Hospital. These lesions were diagnosed pathologically as BSM without atypia in 32 cases, BSM with atypia in 25 cases, dysplasia in 5 cases, carcinoma in situ in 21 cases, microinvasion to the bronchial wall in 4 cases, and stage I well differentiated squamous cell carcinoma in 32 cases. The specimens were fixed with 10% formalin and embedded in paraffin.

2.2. Immunohistochemistry

Mouse monoclonal antibodies against human E-cadherin (HECD-1; Takara, Kyoto, Japan), α-catenin and β-catenin (anti-α-catenin and anti-β-catenin; Transduction Laboratories, Lexington, KY), and plakoglobin (CBL175; Cymbus Bioscience, Southampton, UK) were used for immunohistochemical staining. Four-micrometer-thick tissue sections were prepared from all paraffin-embedded specimens and collected on silane-coated glass slides. After deparaffinization, the formalin-fixed paraffin-embedded sections were treated with

0.01% trypsin and subjected to microwave antigen retrieval [37].

The immunohistochemical method using the avidin-biotin-peroxidase complex was described previously [35]. The reaction products were visualized with diaminobenzidine and the sections were counterstained with hematoxylin.

Negative control staining, which was performed with the same class of immunoglobulin instead of the first antibody, yielded negative results in all cases. The intensity and pattern of immunostaining with HECD-1, anti-α-catenin, anti-β-catenin, and CBL175 in intrabronchial lesions were compared with those of normal bronchial epithelium, and the immunohistochemical staining results were evaluated as described previously [35]. Levels of immunostaining were evaluated in separate compartments of the bronchial epithelium: the basal layer (the first two-fifths of the distance between the basement membrane and the free surface), the intermediate layer, and the superficial layer (the upper one-fifth of this distance). Expression of E-cadherin, α-catenin, β-catenin, and plakoglobin in each layer was judged to be normal if more than 90% of the intrabronchial lesion cells were positively stained by the appropriate antibodies. If staining was distinctly weaker than that of normal epithelium, or if less than 90% of the intrabronchial lesion cells were positively stained, the expression was judged to be reduced. Immunohistochemical staining was scored independently by two observers (Y.K., Y.E.).

2.3. Statistical analysis

The data were analyzed using the Cochran–Armitage test [38], which was conducted by a stepwise method excluding E-cadherin, α-catenin, β-catenin, and plakoglobin, since these four variables are the variables of interest. Differences at $p < 0.05$ were considered to be statistically significant.

3. Results

In bronchial epithelium, E-cadherin and all catenins were expressed at a high level. Immunohistochem-

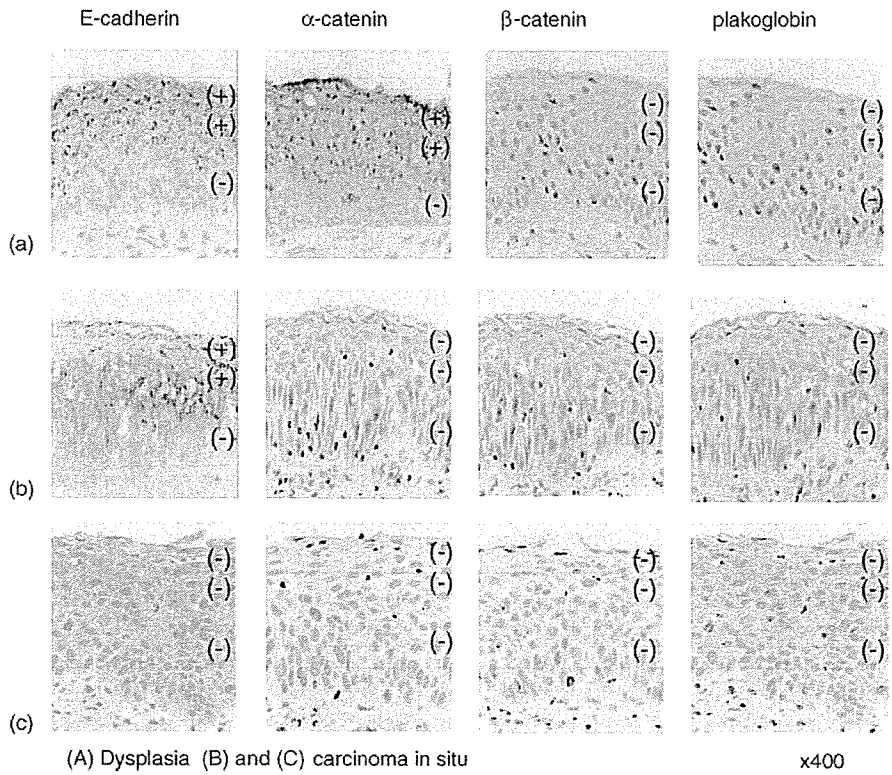

Fig. 1 (A) Representative immunohistochemical staining for E-cadherin, α-catenin, β-catenin, and plakoglobin in biopsy specimens of dysplasia (a) and carcinoma in situ (b and c). Evaluation for each layer of the intrabronchial lesions is shown at the right side of each picture ×400. (B) A borderline area between carcinoma in situ and dysplasia. Evaluation for each layer of the carcinoma in situ area is shown at the left side of each picture, and that for each layer of the dysplasia area at the right side of each picture.

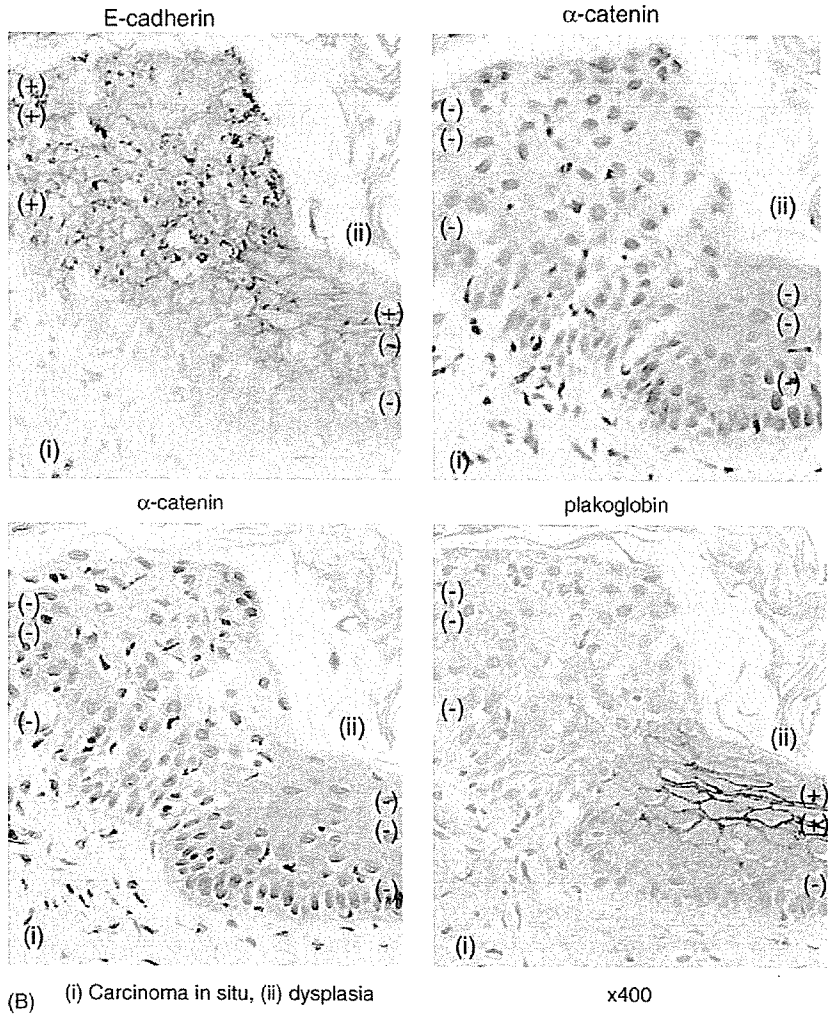

Fig. 1 (*Continued*).

ical findings for representative intrabronchial lesions are shown in **Fig. 1**. Cases with reduced expression of either E-cadherin or catenins in intrabronchial lesions are summarized in **Table 1**. Reduced expression of E-cadherin and/or catenins was closely correlated with an atypical grade of dysplasia in the basal layer ($p < 0.05$). In particular, down-regulation of E-cadherin and/or catenins was associated with an atypical grade of BSM with atypia in intrabronchial lesions ($p < 0.01$). Additionally, reduced expression of E-cadherin and catenins was observed in squamous cell carcinoma, as shown in **Table 2**.

In BMS without atypia ($n = 32$ cases), loss of expression of α-catenin, β-catenin or plakoglobin was observed in the basal layer in six cases (18%), in the intermediate layer in two cases (6%), and in the superficial layer in three cases (9%). In BSM with atypia ($n = 25$ cases), loss of expression of E-cadherin, α-catenin, β-catenin or plakoglobin was observed in the basal layer in seven cases (28%), in the intermediate layer in seven cases (28%), and in the superficial layer in five cases (20%). In dysplasia ($n = 5$ cases), loss of expression of these molecules was observed in the basal layer in two cases (40%), in the intermediate layer in one case (20%), and in the superficial layer in one case (20%). In carcinoma in situ ($n = 21$ cases), loss of expression was observed in the basal layer in 10 cases (48%), in the intermediate layer in 9 cases (43%), and in the superficial layer in 8 cases (38%). In microinvasion to bronchial wall ($n = 4$), loss of expression was observed in the basal layer in four cases (100%), in the intermediate layer in three cases (75%), and in the superficial layer in two cases (50%). These results are presented in **Fig. 2** and **Table 3**.

Table 1 Aberrant expression of E-cadherin and catenins in intrabrounchial lesions

	E-cadherin			α-Catenin			β-Catenin			Plakoglobin			Rate[a] (%)
	B	I	S	B	I	S	B	I	S	B	I	S	
BSM without atypia $n=32$	+	+	+	−	−	+	+	+	+	−	−	−	21
	+	+	+	+	+	+	−	+	+	+	+	+	
	+	+	+	+	+	+	−	+	+	+	+	+	
	+	+	+	+	+	+	+	+	−	+	+	+	
	+	+	+	+	+	+	+	+	+	−	+	+	
	+	+	+	+	+	+	+	+	+	−	+	+	
	+	+	+	+	+	+	+	+	+	−	−	−	
BSM with atypia $n=25$	−	−	+	+	+	+	+	+	+	+	+	+	28
	+	+	+	−	+	+	−	−	−	+	+	+	
	+	+	+	−	−	−	−	−	−	+	+	+	
	+	+	+	+	+	+	−	−	−	+	+	+	
	+	+	+	+	+	+	−	−	−	+	+	+	
	+	+	+	+	+	+	−	−	+	−	−	+	
	−	−	−	−	−	−	−	−	−	−	−	−	
Dysplasia $n=540\%$	−	+	+	−	+	+	−	−	−	−	−	−	40
	−	+	+	−	+	+	+	+	+	+	+	+	
	+	+	+	+	+	+	−	−	+	+	+	+	
	+	+	+	+	+	+	−	+	+	−	+	+	
	+	+	+	−	−	−	−	−	−	−	−	−	
	+	−	+	−	−	+	−	−	−	+	+	+	
Carcinoma in situ $n=21$	−	+	+	−	−	−	−	−	−	−	−	−	48
	−	−	+	−	−	−	+	+	+	+	+	+	
	−	−	−	−	−	+	−	−	−	−	−	+	
	−	−	−	−	−	−	−	−	−	+	+	+	
	−	−	−	−	−	−	−	−	−	−	−	−	
	−	−	−	−	−	−	−	−	−	−	−	−	
Microinvasion to bronchial wall $n=4$	+	+	+	−	−	+	−	−	−	+	+	+	100
	+	+	+	−	−	+	−	−	+	+	+	+	
	+	+	+	+	+	+	−	−	−	−	−	−	
	+	+	+	+	+	+	+	+	+	−	+	+	

Variable	Contrast	*p*-Value
BSM without atypia	BSM with atypia	0.097
BSM without atypia	Dysplasia	0.043
BSM without atypia	Carcinoma in situ	0.003
BSM without atypia	Microinvasive to bronchial wall	0.001

B: basal layer; I: intermedtate layer; S: superficial layer.
[a] Reduced expession rate of either E-cadherin or catenins in intrabronchial lesions.

Table 2 Reduced expression rate of E-cadherin and catenins in advanced stage of squamous cell carcinoma

	Squamous cell carcionoma, $n=32$
E-cadherin	21 (67%)
α-Catenin	26 (81%)
β-Catenin	27 (84%)
Plakoglobin	14 (44%)
Rate[a]	100%

[a] Reduced expression rate of either E-cadherin or catenins in squamous cell carcinoma.

4. Discussion

It has been established that malignant transformation can arise from an accumulation of genetic alterations. This stepwise transformation is known as multistep carcinogenesis. In general, it is known that primary lung carcinoma is one of the most malignant solid tumors, and that it has a wide range of invasive and metastatic behavior. There is a high possibility that alterations in genotype are reflected in the morphological phenotype of the bronchial epithelium. In this context, bronchial

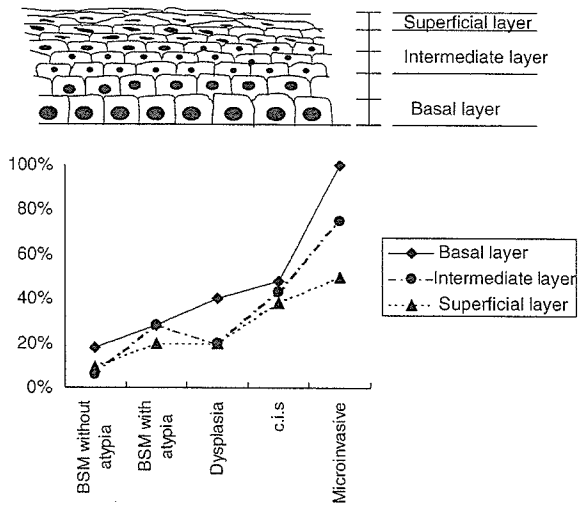

Fig. 2 Proportion of cases with reduced expression of either E-cadherin or catenins within the basal layer (♦), the intermediate layer (●) or the superficial layer (▲) of the intrabronchial lesions. The relative distribution of the different layers is shown in the upper part of the figure.

squamous metaplasia and dysplasia can be considered as precancerous lesions, mutation of the p53 tumor suppressor gene, and deletion of chromosome 17p have been reported in such lesions [39–42]. We have reported sequential changes in cell proliferation, DNA aneuploidy and accumulation of mutant p53 protein during carcinogenesis in the bronchial epithelium, and that these histochemical changes initially occurred in the basal layer [43]. We believe that the ability of cancerous cells to invade the bronchial wall will be acquired in a sequential manner during carcinogenesis. Therefore, we investigated the reduction of expression of E-cadherin and/or catenins in intrabronchial precancerous lesions and the early stages of bronchial squamous cell carcinoma. In intrabronchial lesions and squamous cell carcinoma, expression of either E-cadherin or catenins was reduced in 21% of BSM without atypia, 28% of BSM with atypia, 40% of dysplasia, 48% of carcinoma in situ, 100% of carcinoma microinvasive to the bronchial wall, and 100% of squamous cell carcinoma. We also demonstrated a positive correlation between the expression of these molecules and the grade of atypia of intrabronchial lesions. Our previous studies showed that reduced expression of E-cadherin and catenins occurs frequently in non-small cell lung carcinoma [35]. Hence, our present findings indicate that downregulation of E-cadherin and catenins may play an important role in the progression of human intrabronchial lesions and squamous cell carcinoma.

Studies on cell–cell adhesion molecules may help to clarify the mechanisms of local invasion and metastasis. Investigations of the cadherin–catenin complex have been carried out at the cellular and molecular levels [14,22,44]. It has already been reported that reduction of E-cadherin expression is caused by mutation and by inactivation of the E-cadherin gene by hypermethylation in the promoter region [45]. Dysfunction of the cadherin–catenin complex caused by reduction of the expression of these molecules implies an increased ability of cancer cells to disperse, which is the probable early step of local invasion and metastasis. Reduction of expression of E-cadherin and α-catenin is associated with local invasion and metastasis of scirrhous carcinoma in gastric cancer, breast cancer, and esophageal cancer [20,22].

In BSM with atypia and dysplasia, cells showing reduction of E-cadherin and/or catenin expression were localized mainly in the basal layer. As histological atypia increased, reduced expression of each molecule also became evident in the intermediate and superficial layers. This observation parallels the finding that proliferating cells and cells with accumulation of mutant p53 protein appeared from the basal layer to the superficial layer during carcinogenesis in the bronchus [43]. Therefore, we hypothesize that these cellular changes indicate an increased risk of eventual malignant transformation, and also that cells in the basal layer are the first to acquire the capacity for local invasion.

Our present study suggests that reduction of expression of E-cadherin and/or catenins is a rela-

Table 3 Aberrant expression rate of E-cadherin and/or catenins in intrabronchial lesions

	BSM without atypia	BSM with atypia	Dysplasia	c.i.s	Microinvasion to bronchial wall	Sq.c.ca.
Basal layer	6 (18%)	7 (28%)	2 (40%)	10 (48%)	4 (100%)	100%
Intermediate layer	2 (6%)	7 (28%)	1 (20%)	9 (43%)	3 (75%)	
Superficial layer	3 (9%)	5 (20%)	1 (20%)	8 (38%)	2 (50%)	
Whole layer	7 (21%)	7 (28%)	2 (40%)	10 (48%)	4 (100%)	
Total (cases)	32	25	5	21	4	32

tively early event in the genesis of bronchial squamous cell carcinoma, and that increasing histological atypia is accompanied by further diminution in the expression of these molecules. Finally, reduced levels of E-cadherin and/or catenins might play a critical role in local invasion beyond the basement membrane and the development of the advanced stage of squamous cell lung carcinoma.

References

[1] Takeichi M. Functional correlation between cell adhesive properties and some cell surface proteins. J Cell Biol 1997;75:464–74.

[2] Takeichi M. Cadherin cell adhesion receptors as a morphogenetic regulator. Science 1991;251:1451–5.

[3] Hirano S, Nose A, Hatta K, Kawakami A, Takeichi M. Calcium dependent cell-cell adhesion molecules (cadherins). J Cell Biol 1987;105:2501–10.

[4] Ozawa M, Ringwald M, Kemler R. The cytoplasmic domain of the cell adhesion molecule uvomorulin associates with three independent proteins structurally related in different species. EMBO J 1989;8:1711–7.

[5] Peifer M, McCrea PD, Green KJ, Weischaus E, Gumbiner BM. The vertebrate adhesive junction proteins α-catenin and plakoglobin and the *Drosophila* segment polarity gene Armadillo form a multigene family with similar proteins. J Cell Biol 1992;118:681–91.

[6] Butz S, Stappert J, Wessing H, Kemler R. Plakoglobin and β-catenin: distinct but closely related. Science 1992;257:1142–4.

[7] Cowin P, Kapprell HP, Franke WW, Tamkun J, Hynes RO. Plakoglobin: a protein common to different kinds of intercellular adhering junctions. Cell 1986;46:1063–73.

[8] Korman NJ, Eyre RW, Klaus-Kovtun V, Stanley JR. Demonstration of an adhering-junction molecule (plakoglobin) in the autoantigens of pemphigus foliacus and pemphigus vulgaris. N Engl J Med 1989;321:631–5.

[9] Behrens J, Mareel MM, Van Roy FM, Birchmeier W. Dissecting tumor cell invasion: epithelial cells acquire invasive properties after the loss of uvomorulin-mediated cell–cell adhesion. J Cell Biol 1989;108:2435–47.

[10] Frixen UH, Behrens J, Sachs M, Eberle G, Voss B, Warda A, et al. E-cadherin-mediated cell–cell adhesion prevents invasiveness of human carcinoma cells. J Cell Biol 1991;113:173–85.

[11] Vleminckx K, Vakaet Jr L, Mareel M, Fiers W, Van Roy F. Genetic manipulation of E-cadherin expression by epithelial tumor cells reveals an invasion suppressor role. Cell 1991;66:107–19.

[12] Hirohashi S. Inactivation of the E-cadherin-mediated cell adhesion system in human cancers. Am J Pathol 1998;153:333–9.

[13] Akimoto S, Ochiai A, Inomata M, Hirohashi S. Expression of cadherin–catenin cell adhesion molecules, phosphorylated tyrosine residues and growth factor receptor-tyrosine kinases in gastric cancer. Jpn J Cancer Res 1998;89:829–36.

[14] Shimoyama Y, Nagafuchi A, Fujita S, Gotoh M, Takeichi M, Tsukita S, et al. Cadherin dysfunction in a human cancer line: possible involvement of loss of α-catenin expression in reduced cell-cell adhesiveness. Cancer Res 1992;52:5770–4.

[15] Oda T, Kanai Y, Shimoyama Y, Nagafuchi A, Tsukita S, Hirohashi S. Cloning of the human α-catenin cDNA and its aberrant mRNA in a human cancer cell line. Biochem Biophys Res Commun 1993;193:897–904.

[16] Hirano S, Kimoto N, Shimoyama Y, Hirohashi S, Takeichi M. Identification of a neural α-catenin as a key regulator of cadherin function and multicellular organization. Cell 1992;70:293–301.

[17] Shimoyama Y, Hirohashi S, Hirano S, Noguchi M, Shimosato Y, Takeichi M, et al. Cadherin cell-adhesion molecules in human epithelial tissue and carcinomas. Cancer Res 1989;49:2128–33.

[18] Shimoyama Y, Hirohashi S. Cadherin intercellular adhesion molecule in hepatocellular carcinomas: loss of E-cadherin expression in an undifferentiated carcinoma. Cancer Lett 1991;57:131–5.

[19] Shimoyama Y, Hirohashi S. Expression of E- and P-cadherin in gastric carcinomas. Cancer Res 1991;51:2185–92.

[20] Ochiai A, Akimoto S, Shimoyama Y, Nagafuchi A, Tsukita S. Frequent loss of α-catenin expression in scirrhous carcinoma with scattered cell growth. Jpn J Cancer Res 1994;85:266–73.

[21] Oka H, Shiozaki H, Kobayashi K, Tahara H, Kobayashi T, Takatsuka Y, et al. Expression of E-cadherin cell adhesion molecules in human breast cancer tissues and its relationship to metastasis. Cancer Res 1993;53:1696–701.

[22] Kadowaki T, Shiozaki H, Inoue M, Tamura S, Oka H, Doki Y, et al. E-cadherin and alpha-catenin expression in human esophageal cancer. Cancer Res 1994;54:291–6.

[23] Schipper JH, Frixen UH, Behrens J, Unger A, Jahnke K, Birchmeier W. E-cadherin expression in squamous cell carcinoma of head and neck: inverse correlation with tumor dedifferentiation and lymph node metastasis. Cancer Res 1991;51:6328–37.

[24] Mayer B, Johnson JP, Leitl F, Jauch KW, Heiss MM, Schildberg FW, et al. E-cadherin expression in primary and metastatic gastric cancer: down-regulation correlates with cellular dedifferentiation and glandular disintegration. Cancer Res 1993;53:1690–5.

[25] Bringuier PP, Umbas R, Schaafsma HE, Kaethaus HF, Debruyne FM, Schalken JA. Decreased E-cadherin immunoreactivity correlates with poor survival in patients with bladder tumors. Cancer Res 1993;55:3241–5.

[26] Mattijssen V, Peters HM, Schalwijk L, Manni JJ, Van't Holf-Grootenboer B, de Mulder PH, et al. E-cadherin expression in head and neck squamous-cell carcinoma is associated with clinical outcome. Int J Cancer 1993;55:580–5.

[27] Umbas R, Isaacs WB, Bringuier PP, Schaafsma HE, Karthaus HF, Oosterhof GO, et al. Decreased E-cadherin expression is associated with poor prognosis in prostate cancer. Cancer Res 1994;15:3929–33.

[28] Nakanishi Y, Ochiai A, Akimoto S, Kato H, Watanabe H, Tachimori Y, et al. Expression of E-cadherin, alpha-catenin, beta-catenin, and plakoglobin in esophageal carcinomas and its prognostic significance: immunohistochemical analysis of 96 lesions. Oncology 1997;54:158–65.

[29] Riggleman B, Wieschaus E, Schedl P. Molecular analysis of the armadillo locus: uniformly distributed transcripts and a protein with novel internal repeats are associated with a *Drosophila* segment polarity gene. Genes Dev 1989;3:96–113.

[30] Peifer M, Rauskob C, Willams M, Riggleman B, Wieschaus E. The segment polarity gene armadillo interacts with the wingless signaling pathway in both embryonic and adult pattern formation. Development 1991;111:1029–43.

[31] Oyama T, Kanai Y, Ochiai A, Akimoto S, Oda T, Yanagihara K, et al. A truncated β-catenin disrupts the interaction be-

tween E-cadherin and α-catenin: a cause of loss of intercellular adhesiveness in human cancer cell lines. Cancer Res 1994;54:6282–7.
[32] Hoschuetzky H, Aberle H, Kemler. β-Catenin mediates the interaction of the cadherin–catenin complex with epidermal growth factor receptor. J Cell Biol 1994;127:1375–80.
[33] Ochiai A, Akimoto S, Kanai Y, Shibata T, Oyama T, Hirohashi S. c-erbB-2 gene product associates with catenins in human cancer cells. Biochem Biophys Res Commun 1994;205:73–8.
[34] Kanai Y, Ochiai A, Shibata T, Oyama T, Ushijima S, Akimoto S, et al. c-erbB-2 gene product directly associates with β-catenin and plakoglobin. Biochem Biophys Res Commun 1995;208:1067–72.
[35] Shibanuma H, Hirano T, Tsuji K, Wu Q, Sherestha B, Konaka C, et al. Influence of E-cadherin dysfunction upon local invasion and metastasis in non-small cell lung cancer. Lung Cancer 1998;22:85–95.
[36] Tsuji K, Hirano T, Shibanuma H, Okada S, Kawate N, Konaka C, et al. Cytologic features based on the expression of E-cadherin and catenins in lung adenocarcinoma. Acta Cytologica 1998;43:381–9.
[37] Barbareschi M, Girlando S, Mauri MF, Forti S, Eccher C, Mauri FA, et al. Quantitative growth fraction evaluation with MIB1 and Ki67 antibodies in breast carcinomas. Am J Clin Pathol 1994;102:171–5.
[38] Armitage P. Test for linear trend in proportions and frequencies. Biometrics 1955;11:375–84.
[39] Sundaresan V, Ganly P, Hasleton P, Rudd R, Sinha G, Bleehen NM, et al. p53 and chromosome 3 abnormalities, characteristic of malignant lung tumor, are detectable in preinvasive lesions of the bronchus. Oncogene 1992;7:1289–997.
[40] Sozzi G, Moizzo M, Donghi R, Pilotti S, Cariani CT, Pastorino U, et al. Deletions of 17p and p53 mutations in preneoplastic lesions of the lung. Cancer Res 1992;52:6079–82.
[41] Klein N, Vignaud M, Sadmi M, Plenat J, Borelly J, Duprez A, et al. Squamous metaplasia expression of protooncogenes and p53 in lung cancer patients. Lab Invest 1993;68:26–32.
[42] Nuorva K, Soini Y, Kamel D, Autio-Harmainen H, Risteli L, Risteli J, et al. Concurrent p53 expression in bronchial dysplasia and squamous cell lung carcinoma. Am J Pathol 1993;142:725–32.
[43] Hirano T, Franzén B, Kato H, Ebihara Y, Auer G. Genesis of squamous cell lung carcinoma: sequential change of proliferation, DNA ploidy, and p53 expression. Am J Pathol 1994;144:296–302.
[44] Nose A, Nagafuchi A, Takeichi M. Expressed recombinant cadherins mediate cell sorting in model systems. Cell 1998;54:992–1001.
[45] Yoshiura K, Kanai K, Ochiai A, Shimoyama Y, Sugimura T, Hirohashi S. Silencing of the E-cadherin invasion-suppressor gene by CpG methylation in human carcinomas. Proc Natl Acad Sci USA 1995;92:7416–9.

General Thoracic Surgery

Phase II trial of postoperative adjuvant cisplatin and etoposide in patients with completely resected stage I-IIIa small cell lung cancer: The Japan Clinical Oncology Lung Cancer Study Group Trial (JCOG9101)

Ryosuke Tsuchiya, MD,[a] Kenji Suzuki, MD,[a] Yukito Ichinose, MD,[b] Yoh Watanabe, MD,[c] Tsutomu Yasumitsu, MD,[d] Naoki Ishizuka, PhD,[e] and Harubumi Kato, MD[f]

Objective: Indications for surgical intervention for very limited small cell lung cancer have not yet been determined. The objective of this study is to determine whether resection followed by cisplatin and etoposide is feasible.

Methods: From September 1991 through December 1996, 62 patients with completely resected small cell lung cancer who were less than 76 years of age from 17 centers were entered in the trial. Of 62 patients, 61 were eligible, with a median follow-up of 65 months. Chemotherapy consisted of 4 cycles of cisplatin (100 mg/m^2, day 1) and etoposide (100 mg/m^2, days 1-3). There were 49 (80%) male patients, 44 with clinical stage I disease, 10 with stage II disease, and 6 with stage IIIa disease.

Results: Forty-two (69%) patients received 4 cycles of cisplatin and etoposide. No treatment-associated mortality was noted. Median survival time was not reached in patients with pathologic stage I disease, was 449 days in patients with stage II disease, and was 712 days in patients with stage IIIa disease. Three-year survival was 61% overall, 68% in patients with clinical stage I disease, 56% in patients with stage II disease, and 13% in patients with stage IIIa disease ($P = .02$). Recurrence was noted in 26 (43%) patients overall. Local failure was noted in 6 (10%) patients. Locoregional recurrence tends to be found more frequently in patients with stage IIIA disease. Distant failure was found in 21 (34%) patients overall. Brain metastasis was found in 15% of the patients.

Conclusion: Major lung resection followed by postoperative cisplatin and etoposide is feasible, with a favorable survival profile. Because nodal metastasis appears to be a major prognostic factor, preoperative evaluation of nodal status remains a major concern.

From the Division of Thoracic Surgery,[a] National Cancer Center Hospital, Tokyo; the Department of Thoracic Oncology of the National Kyushu Cancer Center,[b] Kyushu; the Department of Surgery of the University of Kanazawa,[c] Kanazawa; the Department of Surgery of the Habikino Hospital,[d] Osaka; the JCOG Data Center of the National Cancer Center,[e] Tokyo; the Department of Surgery of the Tokyo Medical College,[f] Tokyo, Japan; and the Lung Cancer Surgical Study Group of Japan Clinical Oncology Group.

Supported in part by a Grant-in-Aid for Cancer Research from the Ministry of Health and Welfare.

Received for publication Sept 3, 2003; revisions received April 21, 2004; accepted for publication May 6, 2004.

Address for reprints: Ryosuke Tsuchiya, MD, Thoracic Surgery Division, National Cancer Center Hospital, 1-1, Tsukiji 5 cho-me, Chuo-ku, Tokyo 104-0045 Japan (E-mail: rtsuchiy@ncc.go.jp).

J Thorac Cardiovasc Surg 2005;129:977-83

0022-5223/$30.00

doi:10.1016/j.jtcvs.2004.05.030

The prognosis of lung cancer remains poor, and this disease is the leading cause of cancer mortality worldwide. Small cell lung cancer (SCLC) comprises approximately 20% of lung cancer cases. Without treatment, SCLC has the most aggressive clinical course of any other type of lung cancer, resulting in a very short median survival time of approximately 2 to 4 months. Although surgical resection is generally indicated for early stage non–small cell lung cancer, this is not always the case with SCLC. This can be explained by the fact that

dissemination to regional lymph nodes or distant organs would be found in most patients with SCLC at the time of initial presentation.[1] Therefore, localized forms of treatment, such as surgical resection or radiation therapy, rarely produce long-term survival, and systemic treatment with current chemotherapy regimens is usually incorporated into the treatment program.

Indications for surgical resection for SCLC have not yet been determined, although several authors have reported that a small minority of patients with limited-stage disease and adequate lung function might benefit from surgical resection.[1-9] According to these reports, the prognosis of resected SCLC was not so poor, especially when no pathologic nodal involvement was observed. The 5-year survival ranged from 26% to 61% in these trials if the tumor was stage I. Because SCLC tends to be disseminated and the results of surgical intervention alone for this disease have been reported to be poor,[1,10] postoperative chemotherapy has been used in most studies. However, the chemotherapy was not standardized, and various chemotherapy protocols were often used. Furthermore, most previous studies were retrospective and thus suffered from the inherent weakness of any retrospective assessment of a given treatment.

Because the combination of cisplatin and etoposide has been considered to be standard in the treatment of SCLC,[11] this combination was selected as a postoperative adjuvant regimen. We conducted a prospective study of surgical resection plus adjuvant chemotherapy for stage I through IIIA SCLC to investigate the efficacy of this treatment strategy.

Patients and Methods

Eligibility

Patients who were given postoperative diagnoses of SCLC histologically or cytologically were eligible for enrollment in the study. The patients had to have completely resected pathologic stage I, II, or IIIA disease according to the TNM classification of the International Union Against Cancer.[12] Histologic typing was determined according to the World Health Organization classification.[13] Inclusion criteria included an Eastern Cooperative Oncology Group performance score of 0 or 1, age between 20 and 75 years, no prior treatment for lung cancer, no other concurrent or previous malignancies, a leukocyte count of greater than 3500/μL, a platelet count of greater than 100,000/μL, a hemoglobin level of greater than 9.5 g/dL, a serum creatinine level of less than 1.5 mg/dL, and aspartate aminotransferase–alanine aminotransferase values of less than twice the institutional upper limit of normal. Exclusion criteria included a history of myocardial infarction within the past 3 months, hepatic cirrhosis, and/or severe cardiopulmonary dysfunction that required oxygen therapy. The following preoperative investigations were performed before entry into the study: computed tomographic (CT) scanning of the chest, upper abdomen, and brain; bronchoscopy; chest plain film; radionuclide bone scanning; complete blood cell count and serum chemistry; and physical examination. Preoperative mediastinoscopy was performed in some cases. All patients provided written informed consent before entering the study.

Treatment Schedule

Major lung resection, such as pulmonary lobectomy or pneumonectomy, was required as a surgical procedure for SCLC. Complete hilar and mediastinal lymph node dissections were recommended on the basis of the lymph node map defined by Naruke and colleagues.[14] After confirming complete resection and histologic typing of SCLC histologically, eligible patients were registered in the study.

Chemotherapy consisted of cisplatin (100 mg/m^2 on day 1) and etoposide (100 mg/m^2 on days 1-3; PE regimen). This regimen was repeated every 4 weeks and was administered in 4 courses. The dose was modified according to the blood cell count and renal function on the day of chemotherapy. Chemotherapy was administered unless the leukocyte count was less than 3000/μL or the platelet count was less than 75,000/μL. Chemotherapy was withheld until the counts recovered. If grade 4 hematologic toxicity, according to World Health Organization (WHO) criteria,[15] was seen, the dose of etoposide was reduced to 75%. Chemotherapy was permanently discontinued at any time when the serum creatinine level was 2.0 mg/dL or greater or the blood urea nitrogen level was 30 mg/dL or greater. To assess toxicity, we subjected all patients to complete blood cell counts and blood chemistry evaluations, such as for aspartate aminotransferase–alanine aminotransferase, blood urea nitrogen, and serum creatinine, as well as chest plain film and urinalyses at least once per week during treatment. Toxicity criteria were evaluated on the basis of the WHO criteria.[15]

Patients were followed up at the outpatient department every 3 months postoperatively and underwent CT scans of the chest, upper abdomen, and brain, as well as radionuclide bone scanning every 6 months, even when they were asymptomatic. No postoperative radiotherapy was applied until relapse was apparent.

Sites of relapse were determined by clinical, radiologic, or histologic criteria at initial recurrence. Local failure was defined as recurrence at the primary lung site or hilar-mediastinal lymph nodes. Distant failure was defined as recurrence in the contralateral lung, bone, brain, liver, or other extrathoracic regions.

Statistical Analysis

The trial was designed as a prospective phase II trial. The primary goal of the study was to estimate the survival. A sample size of 30 was considered to provide a power of 90% for detecting a significant improvement in the 3-year survival (from 20% to 50%) in a 1-sided test with an α value of .025 and a β value of .10. The median follow-up period for 35 surviving patients was 65 months. The length of survival was defined as the interval in months between the day of surgical resection of lung cancer and the date of death from any cause or the last follow-up. The survival curves were constructed by using the Kaplan-Meier method,[16] and curves were compared with the log-rank test.

Results

Patient Characteristics

Between September 1991 and December 1996, 62 patients were entered in this phase II trial at the 16 institutions that

TABLE 1. Patient characteristics

Total	61
Sex	
Male	49
Female	12
Age (y)	
Range	22-74
Median	64
Histologic subtype defined by WHO*	
Oat cell type	9
Intermediate type	45
Combined type	7
Clinical stage	
I	44
II	9
IIIA	8
Side of primary tumor	
Right	32
Left	29
Operative procedure	
Lobectomy	57
Pneumonectomy	4
Extent of lymph node dissection†	
Complete hilar and mediastinum	59
Only hilar	2
Pathologic stage	
I	35
II	8
IIIA	18
Performance status	
0	32
1	29

*Histologic subtyping was determined on the basis of the World Health Organization (WHO) classification. †The extent of lymph node dissection was defined by Naruke and associates.[14]

participated in the study. One patient was excluded because his final histologic category was changed from SCLC to large cell carcinoma. Thus, 61 patients were eligible for assessment of survival data, and their characteristics are shown in Table 1. The median age was 64 years (range, 22-74 years). According to histologic typing defined by the WHO, oat cell, intermediate, and combined types were found in 9, 45, and 7 patients, respectively. Forty-four patients had clinical stage I disease, 9 had stage II disease, and 8 had stage IIIA disease. Pathologically, stage I, II, and IIIA disease was found in 35, 8, and 18 patients, respectively.

Treatment Administration

As a surgical procedure, pulmonary lobectomy was performed in 57 (93%) patients, and pneumonectomy was performed in the other 4 patients. Among 4 pneumonectomies, 3 were on the left side, and 1 was on the right side. Complete hilar and mediastinal lymph node dissection was performed in 59 (97%) patients.

TABLE 2. Treatment delivery

Total no. of patients	61
No. of chemotherapy courses	
0	1 (2%)
1	5 (8%)
2	8 (13%)
3	5 (8%)
4	42 (69%)

A total of 204 courses were administered (Table 2). Forty-two (69%) patients underwent a full course of chemotherapy. The other 19 patients did not complete postoperative chemotherapy because of progressive disease in 3 patients, adverse effects in 7 patients, refusal of chemotherapy in 8 patients, and death from pneumonia in 1 patient.

Treatment-Related Toxicity

No treatment-associated deaths were found. Postoperative bronchopulmonary fistula was found in 1 (2%) patient who underwent pulmonary lobectomy after completion of the first cycle of chemotherapy. Chemotherapy-related toxicity is shown in Table 3. Grade 4 toxicity was found in 9 (15%) patients: leukopenia in 4 patients, thrombocytopenia in 2 patients, nausea in 2 patients, and cardiac failure in 1 patient. One patient died of pneumonia 2 months after the first course of chemotherapy, but this was not considered to be chemotherapy related.

Survival

Survival data are shown in Table 4. Among the 61 eligible patients, 35 were still alive after a median follow-up of 65

TABLE 3. Chemotherapy-related toxicity in 60 eligible patients treated for resected stage I to IIIA SCLC

	WHO grade				
Toxicity	1	2	3	4	4 (%)
Anemia	9	29	16	0	0
Leukocytopenia	7	17	26	4	6.5
Thrombocytopenia	11	8	14	2	3.2
Infection	2	1	0	0	0
Nausea	24	13	13	2	3.3
Diarrhea	8	2	2	0	0
Azotemia	35	0	0	0	0
Renal failure	18	0	0	0	0
Stomatitis	14	1	1	0	0
Dyspnea	5	0	0	0	0
Fever	10	7	0	0	0
Skin	4	2	0	0	0
Alopecia	13	23	11	0	0
Cardiac dysfunction	5	2	1	1	1.7
CNS	1	1	1	0	0
Peripheral neuropathy	5	1	0	0	0

WHO, World Health Organization; *CNS,* central nervous system.

TABLE 4. Survival in patients with resected SCLC who underwent postoperative chemotherapy

	Median survival time (d)	Survival 3 y	Survival 5 y
Clinical stage			
IA	Not reached	70%	66%
IB	Not reached	65%	65%
II	Not reached	56%	56%
IIIA	530	13%	13%
Pathologic stage			
IA	Not reached	78%	73%
IB	Not reached	67%	67%
II	449	38%	38%
IIIA	712	39%	39%

months. The overall estimated 3- and 5-year survivals were 61% and 57%, respectively (Figure 1). The 5-year survival was 66%, 56%, and 13% in patients with clinical stage I, II, and IIIA disease, respectively (Figure 2). Among the 44 patients with clinical stage I disease, 27 were classified as having clinical stage IA disease, and the other 17 were classified as having clinical stage IB disease. There was no significant difference in prognosis between clinical stage IA and IB disease. Similar results were obtained regarding the pathologic stage. Pathologic stage I disease showed a significantly better prognosis (Figure 3). The 5-year survivals in the 23 patients with pathologic stage IA disease and the 12 patients with stage IB disease were 73% and 67%, respectively. No significant differences in survival were observed between patients with pathologic stage IA and IB disease.

Patterns of failure. Recurrence was noted in 26 (43%) patients, and the sites of initial relapse at a median follow-up time of 65 months are shown according to the pathologic stage in Table 5. Recurrence was found in 30% of patients with stage IA disease, 25% of patients with stage IB disease, 50% of patients with stage II disease, and 67% of patients with stage IIIA disease.

Local failure was noted in 6 (10%) patients: 4 in the mediastinal lymph nodes and 2 in the bronchial stump. Locoregional recurrence tended to be found more frequently in patients with stage IIIA disease (22%) than in patients with stage I or II disease. Relapse at the bronchial stump was only seen in patients with stage IIIA disease.

Distant failure was found in 22 (36%) patients overall: 6 (26%) with stage IA disease, 2 (17%) with stage IB disease, 4 (50%) with stage II disease, and 9 (50%) with stage IIIA disease. Distant failure was most frequently noted in the brain, followed by the liver. The incidence of brain metastasis was 15% overall, 17% in patients with stage IA disease, and 11% in patients with stage IIIA disease. Bone metastasis was noted exclusively in patients with stage IIIA disease.

Discrepancy between clinical and pathologic stages. Table 6 shows the relationship between the clinical stage and the pathologic stage. Among 44 patients with clinical stage I disease, only 33 (75%) had pathologic stage I disease, and

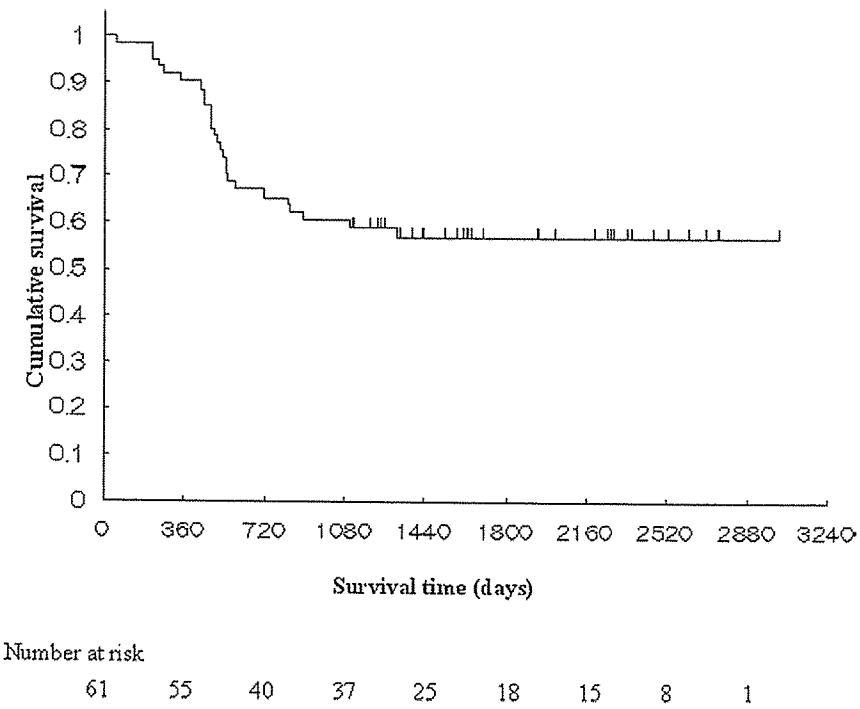

Figure 1. Survival curve for overall patients with resected SCLC.

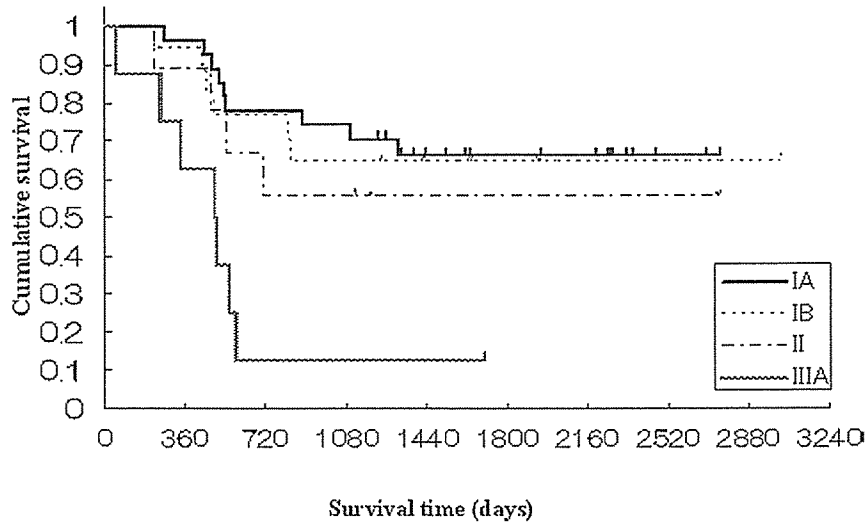

Figure 2. Survival curves for patients with resected SCLC by clinical stages.

6 had stage IIIA disease. Five patients with clinical stage IA disease had mediastinal lymph node metastasis. According to the Bowker test of symmetry, these differences were statistically significant.

Discussion

This phase II trial showed that postoperative PE for patients who underwent surgical resection of stage I to IIIA SCLC was feasible, and the outcome was acceptable. Survival was excellent in patients with stage I disease and did not appear to be inferior to that with chemoradiotherapy in patients with stage II or IIIa disease.

On the basis of the results of the British Medical Research Council, radical radiotherapy has been preferable to surgical intervention for SCLC,[17,18] and the indications for surgical resection for SCLC are still controversial. An operation would be indicated for limited SCLC because the most common relapse site after radiotherapy was locoregional, and surgical intervention might improve local control.[19] Several authors have reported that a small minority of

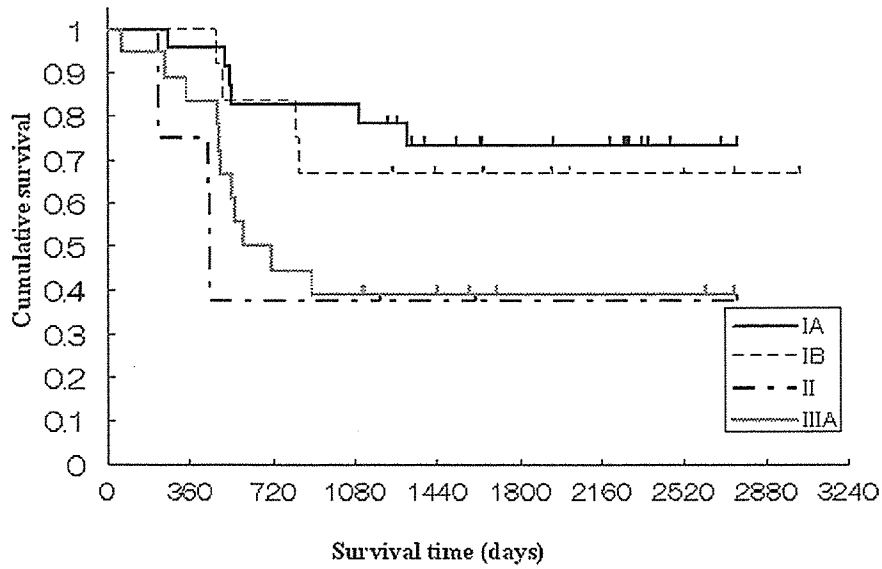

Figure 3. Survival curves for patients with resected SCLC by pathologic stage.

TABLE 5. Site of the first relapse by pathologic stages*

Variables	Overall	Stage IA	Stage IB	Stage II	Stage IIIA
No. of patients	61	23	12	8	18
No. of recurrence	26 (43%)	7 (30%)	3 (25%)	4 (50%)	12 (67%)
Recurrence					
Local					
Overall	6 (10%)	1 (4%)	1 (8%)	0 (0%)	4 (22%)
Mediastinum	4	1	1	0	2
Bronchial stump	2	0	0	0	2
Distant					
Overall	22 (36%)	6 (26%)	2 (17%)	4 (50%)	9 (50%)
Brain	9 (15%)	4 (17%)	0 (0%)	3 (38%)	2 (11%)
Bone	3	0	0	0	3
Liver	7	1	1	1	4
Lung	2	0	1	0	1
Small intestine	2	1	0	0	1

GTS

limited-stage SCLCs could be managed with an operation and postoperative chemotherapy.[1-9] According to those reports, the 5-year survivals were 28% to 36% overall and 26% to 61% in patients with stage I disease. However, most of those reports were retrospective and used various combinations of chemotherapy. Therefore, a prospective trial of adjuvant chemotherapy for patients with resected SCLC using standardized chemotherapy has been needed. Our survival data suggest that postoperative PE after major lung resection and hilar and mediastinal lymph node dissection is a feasible and promising treatment, especially for patients with stage I SCLC. The 3- and 5-year survivals for patients with stage I disease were 78% and 73%, respectively, and the median survival time was not reached. As for patients with stage II or IIIA disease, the results were not definitive, and a further prospective study is needed. This study dealt with postoperatively proved SCLC. As to the indication for surgical intervention for preoperatively diagnosed SCLC, controversies still remain. Our recommendation is as follows. When a patient has SCLC of clinical N1 or N2 status, chemoradiotherapy should be considered because a survival after an operation alone would not be good enough. Surgical intervention should be considered, however, for patients with clinical stage I disease because an operation followed by chemotherapy offers a good prognosis, as shown in this study, and because such SCLC sometimes turns out to be non-SCLC postoperatively. A phase III trial comparing chemoradiotherapy with surgical intervention followed by chemotherapy is interesting. However, the number of patients with SCLC with clinical stage I or II disease is very small, and we do not think it is possible to perform the phase III trial in this population.

TABLE 6. Relationship between clinical and pathologic stages

	Pathologic stage			
Clinical stage	I	II	IIIA	*P* value*
I	33	5	6	.011
II	1	3	5	
IIIA	1	0	7	

**P* value in Bowker's test of symmetry.

Because clinical stage and pathologic stage were significant prognostic factors in our trial, preoperative staging, intraoperative staging, or both should be a major concern for the treatment of very limited SCLC. Actually, the following preoperative investigations were performed before entry into the study in this cohort: CT scans of the chest, upper abdomen, and brain; bronchoscopy; chest plain film; radionuclide bone scans; complete blood cell count and serum chemistry; and physical examination. If the diagnosis of SCLC was made preoperatively, we recommend the same preoperative workup as done by us in this study. Furthermore, if swollen lymph nodes are detected on thoracic CT scans, we absolutely recommend mediastinoscopy for such cases. As for positron emission tomography, we have no recommendation thus far because this modality has recently begun to be evaluated, although it could be useful for staging N1 disease. Intraoperatively, hilar and mediastinal lymph node sampling or dissection was performed in 59 (97%) patients. This intraoperative staging is also important for deciding on the treatment strategy.

The site of the first relapse was another fruit of our study. This clinical trial did not use postoperative mediastinal irradiation or prophylactic cranial irradiation (PCI). We should discuss the importance of these strategies for very limited SCLC. As to locoregional recurrence, approximately 10% of the patients showed relapse in the mediastinal lymph nodes, bronchial stump, or both. Five percent of patients with stage I or II disease eventually have locore-

gional recurrence, whereas this is seen in 22% of patients with stage IIIA disease. These results suggest that patients with stage IIIA disease, at least, could benefit from postoperative mediastinal irradiation, whereas those with stage I or II disease might not need to undergo radiotherapy. Thus, postoperative chemoradiotherapy might be used in a future trial for stage IIIA disease.

Auperin and associates[20] reported that PCI improved both overall survival and disease-free survival among patients with SCLC in complete remission. Surgically resected SCLC would be considered SCLC in complete remission, and PCI would be indicated. Overall, 15% of the patients in our study showed brain metastasis. Even among patients with stage IA disease, more than 10% of the patients had brain metastasis. Therefore, PCI might be necessary for all patients with completely resected SCLC, whereas some authors have insisted that patients with pathologic stage IA SCLC can be cured without any adjuvant treatment.[19]

Noda and coworkers[21] reported that combination chemotherapy consisting of irinotecan (CPT-11) and cisplatin was superior to PE for extensive SCLC. Although concurrent radiotherapy with CPT-11 would be harmful, we would use the new regimen for very limited SCLC, especially for stage II or IIIA SCLC.

Major lung resection with complete hilar and mediastinal lymph node dissection followed by postoperative PE is a feasible treatment and results in a favorable survival profile. Survival was especially good for patients with stage I disease. Our strategy could be used as a standard treatment arm in a future trial for very limited SCLC.

We thank Ms Mieko Imai and Dr Haruhiko Fukuda, JCOG Data Center, National Cancer Center Research Institute, for their technical support in statistical analyses. We also thank Dr Hideo Kunitoh, Medical Oncology and Internal Medicine Division, National Cancer Center Hospital, for his critical discussion.

References

1. Hansen HH, Dombernowsky P, Hirsch FR. Staging procedures and prognostic features in small cell anaplastic bronchogenic carcinoma. *Semin Oncol.* 1978;5:280-7.
2. Davis S, Crino L, Tonato M, et al. A prospective analysis of chemotherapy following surgical resection of clinical stage I-II small-cell lung cancer. *Am J Clin Oncol.* 1993;16:93-5.
3. Hara N, Ichinose Y, Kuda T, et al. Long-term survivors in resected and nonresected small cell lung cancer. *Oncology.* 1991;48:441-7.
4. Karrer K, Shields TW, Denck H, et al. The importance of surgical and multimodality treatment for small cell bronchial carcinoma. *J Thorac Cardiovasc Surg.* 1989;97:168-76.
5. Macchiarini P, Hardin M, Basolo F, et al. Surgery plus adjuvant chemotherapy for T1-3N0M0 small-cell lung cancer: rationale for current approach. *Am J Clin Oncol.* 1991;14:218-24.
6. Shah SS, Thompson J, Goldstraw P. Results of operation without adjuvant therapy in the treatment of small cell lung cancer. *Ann Thorac Surg.* 1992;54:498-501.
7. Shepherd FA, Ginsberg RJ, Evans WK, et al. Reduction in local recurrence and improved survival in surgically treated patients with small cell lung cancer. *J Thorac Cardiovasc Surg.* 1983;86:498-506.
8. Shields TW, Higgins GA Jr, Matthews MJ, et al. Surgical resection in the management of small cell carcinoma of the lung. *J Thorac Cardiovasc Surg.* 1982;84:481-8.
9. Ulsperger E, Karrer K, Denck H. Multimodality treatment for small cell bronchial carcinoma. Preliminary results of a prospective, multicenter trial. The ISC-Lung Cancer Study Group. *Eur J Cardiothorac Surg.* 1991;5:306-10.
10. Martini N, Wittes RE, Hilaris BS, et al. Oat cell carcinoma of the lung. *Clin Bull.* 1975;5:144-8.
11. Fukuoka M, Furuse K, Saijo N, et al. Randomized trial of cyclophosphamide, doxorubicin, and vincristine versus cisplatin and etoposide versus alternation of these regimens in small-cell lung cancer. *J Natl Cancer Inst.* 1991;83:855-61.
12. Hermanek P, Sobin LH. UICC TNM classification of malignant tumours. 4th ed. Berlin: Springer-Verlag; 1992.
13. World Health Organization. Histological typing of lung tumors. 2nd ed. Geneva: World Health Organization; 1981.
14. Naruke T, Suemasu K, Ishikawa S. Lymph node mapping and curability at various levels of metastasis in resected lung cancer. *J Thorac Cardiovasc Surg.* 1978;76:832-9.
15. World Health Organization. WHO handbook for reporting results of cancer treatment. Geneva: World Health Organization; 1979.
16. Kaplan EL, Meier P. Nonparametric estimation for incomplete observations. *J Am Stat Assoc.* 1958;53:457-81.
17. Fox W, Scadding JG. Medical Research Council comparative trial of surgery and radiotherapy for primary treatment of small-celled or oat-celled carcinoma of bronchus. Ten-year follow-up. *Lancet.* 1973; 2:63-5.
18. Comparative trial of surgery and radiotherapy for the primary treatment of small-celled or oat-celled carcinoma of the bronchus. First report to the Medical Research Council by the working-party on the evaluation of different methods of therapy in carcinoma of the bronchus. *Lancet.* 1966;2:979-86.
19. Shepherd FA. Surgical management of small cell lung cancer. In: Pass HI, Mitchell JB, Johnson DH, et al, editors. Lung cancer: principles and practice. Philadelphia: Lippincott, Williams & Wilkins; 2000. p. 967-80.
20. Auperin A, Arriagada R, Pignon JP, et al. Prophylactic cranial irradiation for patients with small-cell lung cancer in complete remission. Prophylactic Cranial Irradiation Overview Collaborative Group. *N Engl J Med.* 1999;341:476-84.
21. Noda K, Nishiwaki Y, Kawahara M, et al. Randomized phase III study of irinotecan (CPT-11) and cisplatin versus etoposide and cisplatin in extensive-disease small-cell lung cancer: Japan Clinical Oncology Group Study (JCOG 9511) [abstract]. *Proc Am Soc Clin Oncol.* 2000;19:482a.

DOI 10.1002/pmic.200401145

Proteomics 2005, *5*, 1150–1159

REGULAR ARTICLE

Clinical-scale high-throughput human plasma proteome analysis: Lung adenocarcinoma

Kiyonaga Fujii[1], *Tomoyo Nakano*[1], *Mitsuhiro Kanazawa*[3], *Shingo Akimoto*[3], *Takashi Hirano*[2], *Harubumi Kato*[2] *and Toshihide Nishimura*[1, 3]

[1] Clinical Proteome Center
[2] Department of Surgery, Tokyo Medical University, Shinjuku, Tokyo, Japan
[3] Medical ProteoScope Co., Ltd., Shinjuku, Tokyo, Japan

Clinical proteomics requires the stable and reproducible analysis of a large number of human samples. We report a high-throughput comprehensive protein profiling system comprising a fully automated, on-line, two-dimensional microflow liquid chromatography/tandem mass spectrometry (2-D μLC-MS/MS) system for use in clinical proteomics. A linear ion-trap mass spectrometer (ITMS) also known as a 2-D ITMS instrument, which is characterized by high scan speed, was incorporated into the μLC-MS/MS system in order to obtain highly improved sensitivity and resolution in MS/MS acquisition. This system was used to evaluate bovine serum albumin and human 26S proteasome. Application of these high-throughput μLC conditions and the 2-D ITMS resulted in a 10-fold increase in sensitivity in protein identification. Additionally, peptide fragments from the 26S proteasome were identified three-fold more efficiently than by the conventional 3-D ITMS instrument. In this study, the 2-D μLC-MS/MS system that uses linear 2-D ITMS has been applied for the plasma proteome analysis of a few samples from healthy individuals and lung adenocarcinoma patients. Using the 2-D and 1-D μLC-MS/MS analyses, approximately 250 and 100 different proteins were detected, respectively, in each HSA- and IgG-depleted sample, which corresponds to only 0.4 μL of blood plasma. Automatic operation enabled the completion of a single run of the entire 1-D and 2-D μLC-MS/MS analyses within 11 h. Investigation of the data extracted from the protein identification datasets of both healthy and adenocarcinoma groups revealed that several of the group-specific proteins could be candidate protein disease markers expressed in the human blood plasma. Consequently, it was demonstrated that this high-throughput μLC-MS/MS protein profiling system would be practically applicable to the discovery of protein disease markers, which is the primary objective in clinical plasma proteome projects.

Received: May 14, 2004
Revised: October 13, 2004
Accepted: November 15, 2004

Keywords:
Clinical Proteomics / Human plasma / Linear ion-trap mass spectrometry / Lung adenocarcinoma / Plasma proteome

Correspondence: Professor Toshihide Nishimura, Professor of Clinical Proteome Center, Tokyo Medical University, 2-6-1, Nishi-shinjuku, Shinjuku-ku, Tokyo 163-0217, Japan
E-mail: nisimura@tokyo-med.ac.jp
Fax: +1-81-3-5321-6624

Abbreviations: ABC, ammonium bicarbonate; **AID-HP**, albumin-and-IgG-depleted human plasma; **IAM**, iodoacetamide; **Ig**, immunoglobulin; **ITMS**, ion-trap mass spectrometry; **μLC**, microflow liquid chromatography; **NSI**, nanoelectrospray ionization; **SCX**, strong cation exchange; **TCEP**, tris[2-carboxyethyl]phosphine; **TPX**, methylpentene polymer

1 Introduction

Human blood plasma is generally the most informative proteome from a medical viewpoint, because it is the primary clinical specimen and it also represents the largest and deepest version of human proteome present in any sample [1–3]. Almost all body cells communicate with the plasma either directly or through tissues/biological fluids, and many of these cells release at least a part of their contents into the plasma upon damage or death. A comprehensive, systematic characterization of the plasma proteome in the healthy and

diseased states will greatly facilitate the development of biomarkers for early disease detection, clinical diagnosis, and therapy of cancer and other diseases. However, broad characterization of the human plasma proteome may pose one of the greatest challenges. This is because it can contain low-level proteins, which are secreted by solid tissues, as well as other important proteins (tissue leakage proteins at pg/mL levels) in the presence of several relatively dominant, high-abundance proteins (particularly HSA at 35–50 mg/mL). The dynamic range of plasma protein concentrations minimally spans nine orders of magnitude. For clinical and diagnostic proteomics using human plasma, it is essential to develop a comprehensive system, which has a high resolution and a wide dynamic range, for large-scale proteome analysis.

Recently, multi-dimensional LC-MS/MS has been developed as a powerful tool, particularly for comprehensive identification of highly complex proteins. This method can achieve a resolving power that is equal to or higher than 2-DE [4–6]. Broad protein identification techniques can detect specific proteins present in low concentrations in a highly complex protein matrix. To characterize the human plasma proteome, Smith *et al.* have achieved a protein identification dynamic range of more than eight orders of magnitude using 2-D LC combined with conventional ion-trap MS/MS instrumentation [6]. This approach has resulted in the identification of >800 plasma proteins from 5 μL plasma without the depletion of highly abundant HSA and/or immunoglobulins (Ig). The multi-dimensional LC-MS/MS techniques reported thus far indicate the potential usefulness of broad protein identification with high resolution and wide dynamic range for cataloging the plasma contents. However, these approaches require further improvement in terms of both ease of use and industrial applicability to routine clinical use, because their application to clinical research requires stable and reproducible analyses of a large number of human samples.

The establishment of a simple, robust, and high-throughput protein profiling system as a global platform is extremely important from the viewpoint of clinical proteomics. This is because a large number of human tissue/biological fluid samples could then be quantitatively analyzed, in a routine and reproducible manner, for expressed proteins. Such a system would help discover any protein that is significantly associated with a specific disease status. We have constructed a technically well integrated and high-throughput LC-MS/MS system with RP microflow LC (μLC) and a conventional ion-trap MS/MS equipped with a nanoelectrospray ionization (NSI) interface to detect lung cancer biomarkers and to analyze apoptotic mechanisms [7, 8]. Additionally, the system has been combined with on- or off-line strong cation-exchange (SCX) chromatography to result in a multi-dimensional protein profiling system. This protein profiling system using off-line 2-D SCX/RP μLC-MS/MS was successfully applied to broad protein identification of human plasma proteins [9]. We have also established protein depletion, in-solution digestion, and data-integrating/mining systems with an automated operation for large-scale human plasma proteome analysis.

The dynamic range and sequence coverage that results from protein identification by LC-MS/MS analysis depends on both the quality of the separation(s) applied and the MS platform [6]. When resolution performance is not considered, the quality of the 2-D LC is substantially related to the number of fractionation steps for the first dimension chromatography and the analytical running time for the second dimension chromatography. Since the dynamic range of the MS platform is based on the performance of the instrument used, the number of the MS/MS acquisition in one run strictly depends on both the scan speed and the analytical time required by the LC-MS/MS analysis. Recently, linear ion-trap MS/MS (2-D ITMS) instruments with a higher scan speed and sensitivity than conventional 3-D ITMS instruments have emerged as new generation instruments. Therefore, we applied the new 2-D ITMS instrument to the fully automated on-line 2-D μLC-MS/MS system developed by us [10].

In this study, we evaluated the performance of the μLC-MS/MS system using the 2-D ITMS instrument for extending the sensitivity, dynamic range, and coverage for comprehensive protein identification. BSA and human 26S proteasome were used as the authentic protein sample and the protein complex sample, respectively. The system, together with the on-line 2-D μLC-MS/MS system, was then applied to proteome analysis of human plasma; HSA- and IgG-depleted samples were obtained from a few healthy individuals and lung adenocarcinoma cases.

2 Materials and methods

2.1 Materials

HPLC-grade ACN, formic acid, and TFA were purchased from Wako Pure Chemical Industries, Ltd. (Osaka, Japan). Milli-Q grade water (Millipore, Bedford, MA, USA) was used. BSA, ammonium formate, ammonium bicarbonate (ABC), and iodoacetamide (IAM) were purchased from Sigma (St. Louis, MO, USA). Human 26S proteasome (PW9310) was obtained from Affiniti Research Products (Devon, UK). Tris[2-carboxyethyl]phosphine (TCEP) was purchased from Pierce (Rockford, IL, USA). Sequencing grade-modified trypsin was purchased from Promega (Madison, WI, USA).

2.2 Preparation of the digested BSA and human 26S proteasome samples

BSA (1 nmol) was diluted with 225 μL ABC (aq., 100 mM); then, 12.5 μL TCEP (10 mM) was added for reduction and the solution mixture was kept at 37°C for 45 min. Further, 12.5 μL IAM (50 mM) was added, and the solution mixture was alkylated in the dark at 24°C for 1 h. The resulting solution was digested with trypsin (trypsin:protein = 1:50, w/w),

and the resultant 250 μL solution was incubated in the dark at 37°C for 15 h. In-solution digestion of the 26S proteasome sample was carried out as follows: 26S proteasome sample (50 μg) was diluted with ABC (aq., 50 mM) containing 10% v/v ACN to a final volume of approximately 190 μL. For reduction, 2.5 μL TCEP (10 mM) was added, and the solution mixture was kept at 37°C for 45 min. Subsequently, 2.5 μL IAM (50 mM) was added, and the solution mixture was alkylated in the dark at 24°C for 1 h. For digestion, trypsin (2 μg) was added to 5 μL ABC (50 mM), and 200 μL of the resulting solution was incubated in the dark at 37°C for 18 h. All reactions were performed in methylpentene polymer (TPX) microtubes (Hitech Inc. Tokyo, Japan) using an Eppendorf thermomixer R (Brinkmann, Westbury, NY, USA) for 1.5 mL microtubes; the resulting solution was interval-mixed (10 s) at 850 rpm. The digested 26S proteasome sample (50 μL) was diluted with 125 μL of 2% v/v ACN (aq.) containing 0.005% v/v TFA (aq.) after adjusting the pH to approximately 3 with 50 μL of 1% v/v TFA (aq.); the samples (25 μL) were then injected into the μLC-MS/MS system described in this paper.

2.3 Sample preparation of the digested human plasma protein mixture

The human blood plasma samples treated with heparin were obtained from Tokyo Medical University (Tokyo, Japan) and acquired from three, healthy, anonymous, male donors (samples: H-N, H-I, and H-S) and two male donors who were diagnosed with adenocarcinoma on the basis of clinical and laboratory criteria (stage: IIIA, samples: AC88 and AC94), after obtaining their informed consent. HSA and IgG in the human plasma samples (500 μL) was removed by affinity adsorption chromatography using Bio-Rad's Affi-Gel Blue Gel and protein A column (Bio-Rad Hercules, CA, USA), respectively (details not shown). The final concentration of the resulting HSA- and IgG-depleted human plasma (AID-HP) samples were 4.1 (H-N), 8.6 (H-I), 6.6 (H-S), 5.8 (AC88), and 7.2 mg/mL (AC94) in ABC (25 mM). Subsequently, 100 μL of the AID-HP sample was diluted with 400 μL ABC (25 mM) containing 32% v/v ACN. For reduction, 25 μL TCEP (50 mM) was added and the solution mixture was kept at 37°C for 45 min. Subsequently, 25 μL IAM (250 mM) was added and the solution mixture was alkylated in the dark at 24°C for 1 h. For digestion, trypsin (5 μg) was added and the resulting solution (555 μL) was incubated in the dark at 37°C for 16 h. All these reactions were carried out using the Eppendorf thermomixer R for 1.5 mL TPX microtubes, and the mixing was carried out at 850 rpm with periods and intervals of 10 s each. For the 1-D μLC-MS/MS analysis, the digested AID-HP samples (20 μL) were diluted with 20 μL of 1% v/v TFA (aq.) and 160 μL with 2% v/v ACN (aq.) containing 0.1% v/v TFA, in a TPX auto sampler tube; 20 μL of the resultant samples was injected into the system. In order to prepare individual mixture samples of the healthy and adenocarcinoma groups for 1-D and 2-D μLC-MS/MS analyses, 33.3 μL of each of the three AID-HP samples from the healthy group and 50 μL of each of the two AID-HP samples from the adenocarcinoma group were mixed with 100 μL of 1% v/v TFA (aq.), respectively; subsequently, 4 μL of the resulting sample solutions was used in these analyses.

2.4 1-D RP and 2-D SCX/RP μLC-NSI-MS/MS analyses

The 1-D and 2-D LC-MS/MS system with RP-μLC comprised a Paradigm MS4 dual solvent delivery system (Michrom BioResources, Auburn, CA, USA) for HPLC, an HTS PAL auto sampler with two 10-port injector valves (CTC Analytics, Zwingen, Switzerland), Finnigan LCQ Deca XP plus 3-D ion-trap, and Finnigan LTQ linear ITMS (Thermo Electron, San Jose, CA, USA) equipped with NSI sources (AMR Inc., Tokyo, Japan). Sample injection for the 1-D and 2-D μLC-MS/MS analyses as well as SCX separation for 2-D analysis were automatically carried out using the HTS PAL auto sample injection system with no change in the configurations. The SCX separation was performed on an SCX microtrap cartridge (12 μm, 300 Å, 8 × 1.0 mm i.d., Michrom) by stepwise elution on the first injector valve. The solvent system containing 2% v/v ACN was composed of 0.005% v/v TFA (aq.) and 1 M ammonium formate (aq.) adjusted to pH 2.8 with TFA, and the elution solvents (25, 50, 100, 150, 200, and 500 mM) were prepared by mixing these. The effluent from all the SCX fractions was flowed serially into a peptide CapTrap cartridge (2.0 × 0.5 mm i.d., Michrom), present on the second injector valve, for concentration and desalting. After desalting with 0.1% v/v TFA (aq.) containing 2% v/v ACN, the sample was loaded onto a capillary RP column, MAGIC C_{18} (3 μm, 200 Å, 50 × 0.2 mm i.d., Michrom), for 2-D separation. Digested samples for the 1-D RP analysis were also injected directly into a peptide CapTrap cartridge for concentration and desalting and then applied to RP separation. Solutions of 2% and 90% v/v ACN (aq.) were used as the mobile phases A and B, respectively, and both contained 0.1% v/v formic acid. The gradient conditions in the chromatographic run were as follows: B 5% (0 min) → 65% (20 min) for the digested samples of BSA and 26S proteasome, and B 5% (0 min) → 40% (70 min) → 95% (80 min) for plasma samples. Effluent solvent at 1.0–1.2 μL/min from the HPLC was introduced into the mass spectrometer by the NSI interface *via* an injector valve with a CapTrap cartridge and the RP column. The NSI needle (FortisTip, OmniSeparo-TJ, Hyogo, Japan), which was connected directly to the RP column outlet, was used as the NSI interface and the voltage was 1.8 kV, while the capillary was heated to 200°C [11]. No sheath or auxiliary gas was used. Further, the mass spectrometer was operated in a data-dependent acquisition mode in which MS acquisition with a mass range of m/z 450–2000 was automatically switched to MS/MS acquisition under the automated control of the Xcalibur software. The most intense ion of the full MS scan was selected as the parent ion and it was subjected to MS/MS scan with an isolation width of m/z 2.0; the activation amplitude parameter

was set at 30%. For the human plasma samples, the full MS scan was acquired followed by two successive MS/MS scans of the two most intense precursor ions detected in the full MS scan. The trapping time was 100 ms under the auto gain control mode. Data was acquired using the dynamic mass-exclusion windows that had an exclusion of 3.0-min duration and exclusion mass widths of −0.5 and +1.5 Da.

2.5 Database searches

All MS/MS data were investigated using the Mascot search engine (Matrix Science, London, UK) [12] against the Swiss-Prot database. The data acquired for BSA digests were investigated against other mammalian subsets of the sequences. The MS/MS data of the human 26S proteasome and plasma samples were investigated against the *Homo sapien* subsets of the sequences. The database searches allowed for fixed modification on the cysteine residue (carbamidomethylation, +57 Da), variable modification on the methionine residue (oxidation, +16 Da), peptide mass tolerance at ±2.0 Da, and fragment mass tolerance at ±0.8 Da.

3 Results and discussion

3.1 Evaluation of the μLC-MS/MS analysis using the linear 2-D ITMS instrument

We developed the μLC-MS/MS system with RP separation (1-D RP), which corresponds to the second dimension separation for the on-line and off-line 2-D μLC-MS/MS system [9, 10]. This system comprises a microflow LC system with a variable splitter, a versatile auto-sampler equipped with an injector valve, and a LCQ 3-D (ITMS) with an NSI stage. A flow rate of 1.0–1.2 μL/min *via* the injector valve and the RP column (0.2 mm i.d.) has been adopted as a convenient and efficient condition for routine proteome analysis with high sensitivity and reproducibility. The detection limit for identification of proteins in protein digests was approximately a few fmol. In order to evaluate the sensitivity of the new linear 2-D ITMS instrument (LTQ) for protein identification, we connected our RP μLC system to the LTQ instead of the conventional 3-D ITMS (LCQ) instrument. BSA digests (5–500 fmol) were applied to μLC-MS/MS analysis using the LTQ and LCQ instruments under identical conditions except those used for the mass spectrometer. The base-peak chromatogram for BSA digests (500 fmol) is shown in Fig. 1a. A comparison of the coverage, in terms of protein identification, between the LCQ and LTQ instruments revealed that 25% coverage of the BSA sequence was acquired from 5 fmol of the digests using the LTQ instrument, as shown in Fig. 2. Since the same coverage was obtained from 50 fmol of the digests using the LCQ instrument, the results indicated that the protein identification improved markedly as the sensitivity increased 10-fold using the LTQ instrument.

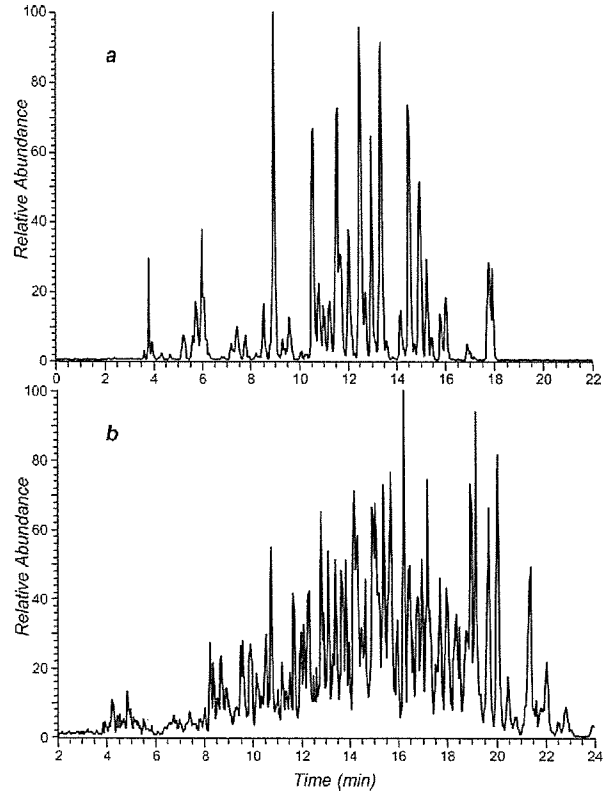

Figure 1. Base-peak chromatograms of the digested BSA (a) and 26S proteasome (b) using 1-D RP μLC-MS/MS analysis.

A dramatic improvement is achieved in the LTQ instrument in terms of the scan speed, which is higher than that of conventional 3-D ITMS instruments. Figures 3a and 3b show the expanded mass chromatograms with stick plotting at *m/z* values 710.0–711.5 obtained by μLC-MS/MS analysis of BSA digests using the LTQ and LCQ instruments, respectively. A stick in the peak represents a single full MS or MS/MS scan. The range denoted by the arrow in Fig. 3 shows that 62 events that carried out the acquisition of a full MS and an MS/MS spectra were achieved by the LTQ instrument in comparison with 12 events acquired by the LCQ instrument in 30 s. When conventional LCQ instruments are used, we usually apply three and two microscans for full MS (50 ms trapping time) and MS/MS (200 ms) accumulations, respectively, in order to obtain a better quality spectrum from a single scan. On the other hand, both spectra for peptide sequencing in protein identification were effectively acquired by one microscan of both full MS (50 ms) and MS/MS (100 ms) accumulations by LTQ instrument. As a result, using the LTQ instrument, it is possible to obtain an approximately five-fold higher number of MS/MS spectra in the same analytical run time.

In general, it is necessary to acquire a greater number of MS/MS spectra for the identification of a greater number of proteins using peptide sequencing. In studies where LC-MS/

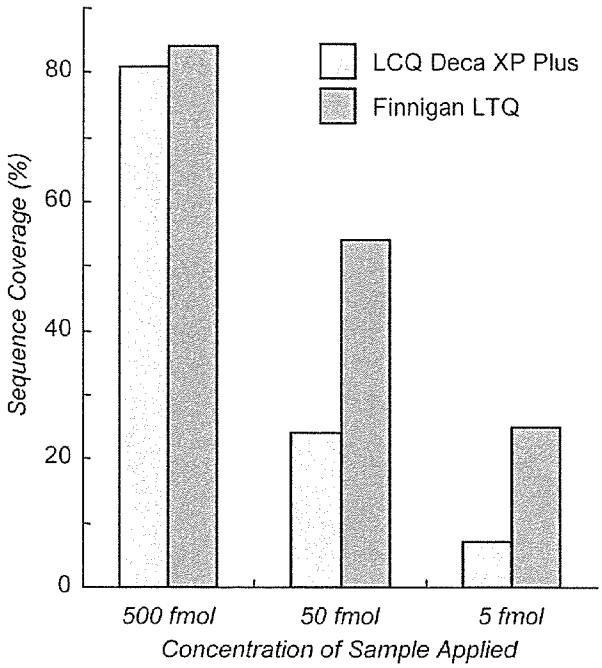

Figure 2. Comparison of sequence coverage of BSA digests (5–500 fmol) by μLC-MS/MS analysis using LCQ Deca XP plus 3-D ion-trap and Finnigan LTQ linear ion-trap MS instruments.

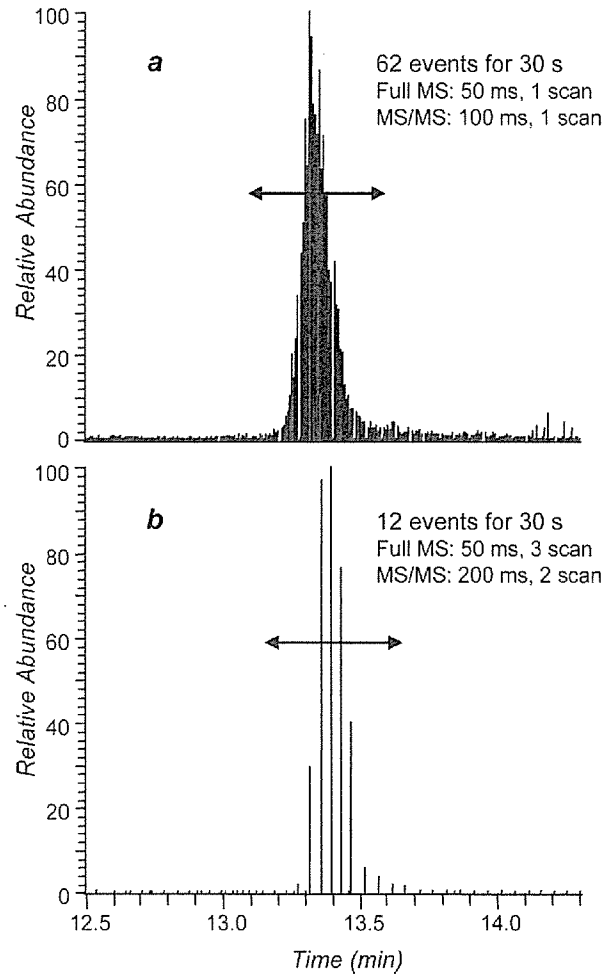

Figure 3. Mass chromatograms at *m/z* 710.0-711.5 by μLC-MS/MS analysis of BSA digests using Finnigan LTQ (a) and LCQ Deca XP plus (b) instruments. A stick in the peak is a single full MS and MS/MS scan of the mass spectrometer, and 62 and 12 events (acquisition of a full MS and a MS/MS in one event) were carried out by the LTQ and LCQ instruments, respectively.

MS was used for comprehensive proteome analysis, several researchers investigated various methods to data-dependently amass MS/MS spectra for a single analysis. These methods include employing a longer analytical time, triple and more MS/MS acquisition against a single full MS spectrum, multiple analyses of the same sample using common conditions or fractionated mass range, etc. While obtaining the MS/MS spectra, the scan speed is a mechanical limitation and a data-dependent scan misses many of the peptide sequences for low abundance peaks that are behind large peaks. Therefore, it is necessary to choose the applications of these techniques for comprehensive proteome analysis of highly complex protein mixtures such as human plasma and whole cell lysates. The drawbacks of clinical proteomics for a large number of human samples are the inability to conduct multiple analyses of the same sample and the longer running time required by the comprehensive LC-MS/MS analysis. Consequently, the performance of the LTQ instrument with a higher scan speed is better than that of the conventional 3-D ITMS instrument, because it enables more informative high-throughput LC-MS/MS analysis for highly complex clinical samples. Therefore, to verify the applicability of LTQ instruments, the human 26S proteasome, which is a highly complex protein mixture consisting of 31 components, was subjected to analysis. As shown in Fig. 1b, equivalent amounts of the digested 26S proteasome sample were analyzed using the LCQ and LTQ instruments under identical μLC conditions. The data-dependent MS/MS acquisition, in which the full MS acquisition is followed by a single MS/MS scan of the most intense precursor ion obtained from the full MS scan, was applied with three microscan full MS (50 ms trapping time) and two microscan MS/MS (200 ms) accumulations for the LCQ, and one microscan of both full MS (50 ms) and MS/MS (100 ms) accumulations for the LTQ instruments. During the 20 min analysis, approximately 450 and 2200 MS/MS spectra were obtained from the 1-D RP μLC-MS/MS analyses using the LCQ and LTQ instruments, respectively. These data were evaluated using a Mascot database search against the Swiss-Prot database, and the search results obtained for the peptide MS/MS assignment were filtered based on the criterion defined as a Mascot peptide score more than 20 and ranked first, described in detail below. Table 1 (see also Supplemen-

Table 1. Protein identification results of human 26S proteasome.

Protein	LCQ Deca XP Plus			Finnigan LTQ		
	Score	Coverage	Peptide	Score	Coverage	Peptide
26S protease regulatory subunits						
PRS4	221	13	3	851	41	16
PRS6	142	9	3	757	48	16
PRS7	348	15	5	1346	55	23
PRS8	299	16	4	1304	58	20
PRSA	377	21	7	1093	53	19
PRSX	154	7	2	715	36	12
Proteasome subunit alpha types						
PSA1	494	36	8	658	48	11
PSA2	261	18	4	569	56	9
PSA3	145	13	3	584	43	11
PSA4	115	9	2	459	33	7
PSA5	158	17	3	483	47	8
PSA6	559	38	8	700	48	11
PSA7	423	35	7	772	57	12
Proteasome subunit beta types						
PSB1	275	34	5	596	53	10
PSB2	256	24	4	456	43	8
PSB3	235	24	3	379	35	5
PSB4	117	9	2	511	48	8
PSB5	528	42	7	670	58	10
PSB6	200	13	3	271	24	5
PSB7	232	14	4	381	33	7
PSB8	ND	ND	ND	180	18	4
26S proteasome non-ATPase regulatory subunits						
PSD1	227	6	3	1636	38	27
PSD2	380	10	6	1386	34	26
PSD3	690	24	10	1445	50	25
PSD4	74	5	1	358	22	6
PSD6	206	12	3	1001	46	18
PSD7	250	15	3	487	42	10
PSD8	ND	ND	ND	228	19	5
PSDB	571	22	8	1445	59	23
PSDC	359	15	5	1147	37	20
PSDD	183	10	4	966	52	17
		Total	130		Total	409

The protein identification data of 31 components consisted of human 26S proteasome including the number of the peptide fragments assigned (Peptide) and the sequence coverage according to these peptides (Coverage). The protein score is calculated by the addition of these peptide scores (Score) in comparison to 1-D μLC-MS/MS analysis using conventional 3-D ion-trap MS (LCQ Deca XP Plus) and new linear ion-trap MS instruments (Finnigan LTQ). ND, not detected.

tary Table A) shows protein identification results including the number of peptide fragments assigned, sequence coverage with these peptides, and the protein score calculated by addition of these peptide scores with respect to the 31 components of the 26S proteasome. In the case of the LTQ instrument, 409 peptide fragments were assigned as components of the 26S proteasome, and this number was approximately three-fold higher than that obtained when the LCQ instrument was used (130 peptide fragments). The individual components of the 26S proteasome were identified by 13.2 and 4.5 peptide fragments, 43.0% and 18.1% sequence coverage, and 821.9 and 292.4 protein scores on an average, using the LTQ and LCQ instruments, respectively. Twenty-nine proteins in 31 components were identified even by the LCQ instruments using our RP μLC system with high-resolution power, as shown in Fig. 1b. However, the peptide fragments of the remaining two components were not observed from the filtered database search results. A number